EFFECT OF VIBRATION FREQUENCY ON NACA 4412 AIRFOIL AERODYNAMIC PERFORMANCE

by

CHAN ZE YU

Thesis submitted in fulfilment of the requirements for the Bachelor Degree of Engineering (Honours) (Aerospace Engineering)

June 2019

ENDORSEMENT

I, Chan Ze Yu hereby declare that all corrections and comments made by the supervisor and examiner have been taken consideration and rectified accordingly.

(Signature of Student)

Date:

(Signature of Supervisor)

Name: Prof. Ir. Dr. Mohd Zulkifly Abdullah
Date:

(Signature of Examiner)

Name: Dr. Norizham Bin Abdul Razak
Date:

DECLARATION

This thesis is the result of my own investigation, except where otherwise stated and has not previously been accepted in substance for any degree and is not being concurrently submitted in candidature for any other degree.

(Signature of Student)

Date:

ACKNOWLEDGEMENTS

Firstly, I would like to express my sincere gratitude to my supervisor and advisor Prof. Ir. Dr. Mohd Zulkifly Abdullah for the enormous support, patience and motivation towards my final year project. His guidance helped me throughout the research and the writing of this thesis.

I would also like to thank Dr. Norizham Bin Abdul Razak for being my examiner to assess this final year report. Also, I would like to appreciate Dr. Nurulasikin Mohd Suhadis for laying out a proper thesis guideline.

Besides, I would like to thank Mr. Muhamad Zulkhairi bin Mat Saad for his assistance on handling the setup of wind tunnel equipment and his insightful comments in this project. Without his assistance it would not be possible to conduct the experiments.

Last but not least, I would like to thank my friends and family for their precious spiritual support throughout the research and my life in general.

EFFECT OF VIBRATION FREQUENCY ON NACA 4412 AIRFOIL AERODYNAMIC PERFORMANCE

ABSTRACT

Vibration is due to the aeroelastic stability of a typical section airplane wing NACA 4412 which finishes in general by the breaking of the plane, it can be determined as a dynamic instability of the structure. As vibration might lead to catastrophe, it is very important to understand the effect of vibration frequency on an airfoil aerodynamic performance. Thus, this project was designed to obtain the aerodynamic characteristics on NACA 4412 airfoil at different vibration frequencies and to study the aerodynamic characteristics on NACA 4412 airfoil at different Reynolds numbers. The experiment was conducted at two different cases, one by using a rigid airfoil without vibration motor attached on it while another case is by using a vibrating airfoil. As known, the performance of an aircraft wing depends mostly on the aerodynamic characteristics such as the lift force, drag force and etc. In this paper, experiment will be conducted in turbulent flow with Reynolds numbers (17 000, 27 000, 34 000, 46 000 and 57 000) at different angles of attack (0 °, 10 °, 20 °, and 30 °) for the two cases mentioned. For the case of using vibration motor, the vibration frequency applied to the airfoil model is varied by the number of rotation of the vibration motor used to the induce vibration. The results will be recorded and plotted to observe how the lift-to-drag ratio of the NACA 4412 airfoil model vary with different vibration frequencies. The effect of varying Reynolds numbers on the aerodynamic characteristics was also investigated in both cases.

KESAN FREKUENSI GETARAN PADA AIRFOIL NACA 4412 TERHADAP PRESTASI AERODINAMIK

ABSTRAK

Getaran adalah disebabkan oleh kestabilan aeroelastik seksyen tipikal sayap pesawat NACA 4412 dan ia boleh ditentukan sebagai ketidakstabilan dinamik struktur. Getaran akan membawa kemalangan yang tidak diingini, oleh itu, kesan frekuensi getaran pada prestasi aerodinamik airfoil perlu dikaji dan difahami. Projek ini direka untuk mendapatkan ciri-ciri aerodinamik pada airfoil NACA 4412 pada frekuensi getaran yang berlainan dan untuk mengkaji ciri-ciri aerodinamik pada airfoil NACA 4412 pada nombor Reynolds yang berbeza. Eksperimen dalam projek ini akan dijalankan dalam dua kes yang berbeza, satu menggunakan model airfoil tanpa motor getaran manakala satu dengan motor getaran dilampirkan pada model airfoil. Seperti yang diketahui, prestasi sayap pesawat bergantung pada ciri-ciri aerodinamik seperti daya angkat, daya seretan dan sebagainya. Dalam makalah ini, eksperimen akan dijalankan dalam aliran turbulen dengan nombor Reynolds (17 000, 27 000, 34 000, 46 000 and 57 000) pada sudut serang yang berlainan (0 °, 10 °, 20 °, dan 30 °) untuk kedua-dua kes tersebut. Bagi kes yang menggunakan motor getaran, frekuensi getaran akan dikawal oleh bilangan putaran yang mendorong getaran tersebut. Keputusan dari kedua-dua eksperimen akan direkodkan dan diperiksa untuk mengkaji bagaimana nisbah daya angkat dengan daya seretan dipengaruhi oleh frekuensi getaran. Kesan pelbagai nombor Reynolds pada ciri-ciri aerodinamik juga akan dikaji dalam kedua-dua kes.

TABLE OF CONTENTS

LIST OF FIGURES

LIFT OF TABLES

LIST OF ABBREVATIONS

AOA : Angle of attack

Re : Reynolds Number

LIST OF SYMBOLS

A	: Area of specimen
c	: Chord length
D	: Drag
L	: Lift
f	: Frequency
μ	: Dynamic viscosity
ρ	: Air density
v	: Air speed
S	: Wing area
C_l	: Lift coefficient
C_d	: Drag coefficient
L/D	: Lift-to-drag ratio
α	: Angle of attack
Re	: Reynolds number

CHAPTER 1

INTRODUCTION

1.1 Research background

Aerodynamics deal with the study of the resulting effects of relative motion between air molecules and body surfaces (Fearn, 2008). The impact of these interactions are due to the forces generated whenever there is relative motion between air molecules and body surfaces. In terms of aerodynamics, the forces mostly encountered are the lift and drag forces (Cengel and Cimbala, 2014) which are most efficiently generated by an airfoil (Kevadiya and Vaidya, 2013). The aerodynamic characteristics of any particular airfoil may be represented by plots showing the amount of lift and drag obtained at various angles of attack as well as the Reynolds number (Petinrin and Onoja, 2017).

Aeroelasticity phenomena involve the study of the interactions between inertial, elastic and aerodynamic forces that occur when an elastic body is exposed to a fluid flow (Panda and S R Pappu, 2009). Vibration is defined as a phenomenon where oscillations occur about an equilibrium point. In terms of aerodynamics, vibration happens due to the dynamic instability of the structure such as the airplane wing. As known, vibration might result in negative influence on the performance of an aircraft, leading to catastrophe (Hodges and Pierce, 2002).

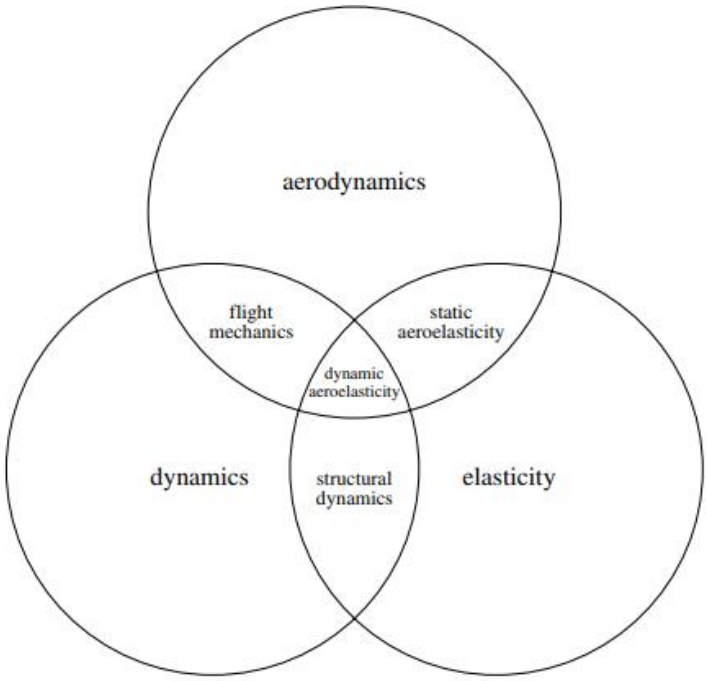

Figure 1. 1: Schematic of the field of aeroelasticity (Hodges and Pierce, 2002)

A flexible structure is now increasingly used in aerospace vehicles due to its adaptability to severe flow conditions resulting in a positive influence on aerodynamic performance. The vibration of a flexible structure causes some complicated phenomena because of its particular wake dynamic structure. As the angle of attack of airfoil increases or decreases beyond a certain limit, vortices start shedding from the trailing edge (Khan et al., 2017) .The vortex pattern can be changed if the airfoil or its surface vibrates in the cross-flow direction. Frequency of vibration plays a crucial role in flow structure downstream of the airfoil especially when the vibration frequency approaches the vortex shedding frequency. It leads to frequency synchronization or lock-in between the two frequencies where the vibration frequency dominates the natural vortex shedding frequency.

However, when a fully flexible structure is at a risk of damage, negative impacts happen such as aerodynamic flutter. An aerodynamic flutter is a very dangerous phenomenon resulting from an interaction between elastic, inertial and aerodynamic forces. This takes place when the structural damping is not sufficient to damp the vibration movements introduced by the aerodynamic effects (Ramdenee et al., 2013). Flutter takes place for any object in an intense fluid flow and condition of positive retroaction. The vibratory movement of any object may increase the aerodynamic solicitation, consequently amplifying the structural vibration.

Vibration induced by the unsmooth runway, noise or the vibration of the aircraft engine might cause negative impact to the aircraft efficiency. To understand the effect of vibration frequency on NACA 4412 airfoil aerodynamic performance, this project conducts the experiment in two cases, one with a vibration motor attached to the airfoil model while the other without the vibration motor. Chapter 1 is an introduction on vibration effect where explanations are provided to highlight the significance of aerodynamic performance and vibration effect on an airfoil. Chapter 2 reviews previously published literature and research surrounding topic of vibration frequency effects on an airfoil. The methodology used for current research is presented in Chapter 3, covering the experimental apparatus, data collection procedures and calibration. Chapter 4 outlines the results obtained and discusses the possible causes and solutions to the problems. Chapter 5 summarizes the overall finding of this research.

1.2 Problem statement

Vibration of wing can affect the aerodynamic characteristics of the aircraft. The aerodynamic performance and airfoil efficiency of a rigid NACA 4412 airfoil model will definitely show some obvious differences from that of a vibrating NACA 4412 airfoil model at different Reynolds numbers and angles of attack. It is important to study the effect of vibration frequency on the airfoil model aerodynamic performance and airfoil efficiency.

1.3 Objectives

This research aims to study the effects of vibration frequency on a NACA 4412 airfoil aerodynamic performance. Thus, it is important to obtain the aerodynamic characteristics on NACA 4412 airfoil at different vibration frequencies. The research also attempts to study the aerodynamic characteristics on NACA 4412 airfoil at different Reynolds numbers. Lastly, the study compares the aerodynamic performance of a vibrating airfoil and the rigid NACA 4412 airfoil model.

1.4 Scope of work

The NACA 4412 airfoil model is to be tested in the wind tunnel at various angles of attack (0 °, 10 °, 20 °, and 30 °) and at high wind speed to obtain the aerodynamic forces such as lift and drag. The second set of experiment will be conducted with the same airfoil model but attached with the vibration motor. The vibrating airfoil model is to be tested at various vibration frequencies manipulated by the number of vibration motors used to obtain the aerodynamic forces. The research is fully experimental.

CHAPTER 2

LITERATURE REVIEW

Forces acted on an aircraft in flight includes lift, weight, thrust and drag as shown in Figure 2.1. The weight of an aircraft that is always directly towards the Earth's center depends on its size and materials as well as the payload or fuel it carries. As for the thrust that directs forward along the center line of the aircraft, it can be determined by the size and type of propulsion system of the airplane. Lift and drag are important aerodynamic forces that depend on the shape and size of the aircraft, air conditions and flight velocity. As shown in the Figure 2.1, lift is directed perpendicular to the flight path whereas drag is directed along the flight path (Hall, 2015a).

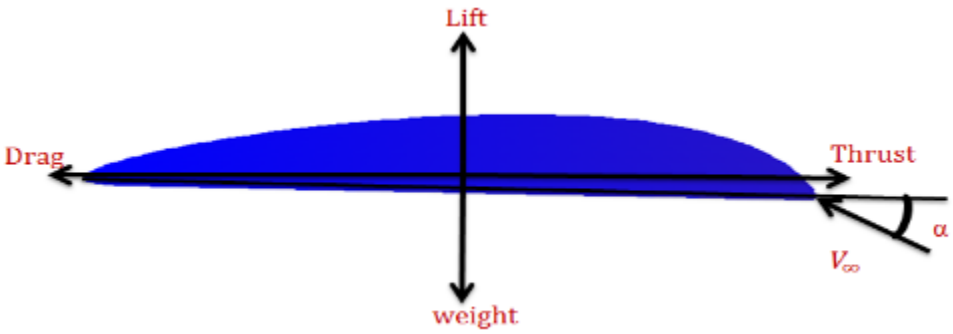

Figure 2. 1: Forces on an aircraft where α is the angle of attack and V_∞ is the relative wind velocity (Nair, 2014)

Since the lift and drag are both aerodynamic forces, the lift-to-drag ratio or L/D ratio indicates the aerodynamic efficiency of the airplane. The higher the L/D ratio of an aircraft, the larger the amount of lift generated or the smaller the amount of drag generated (Hall, 2015a). Maximum lift-to-drag ratio is one of the most important performance parameters of

an aircraft (Gudmundsson, 2014). Also, it can be said that the higher the lift-to-drag ratio of an airfoil, the higher the airfoil efficiency. Figure 2.2 shows the forces acting on a typical airfoil section.

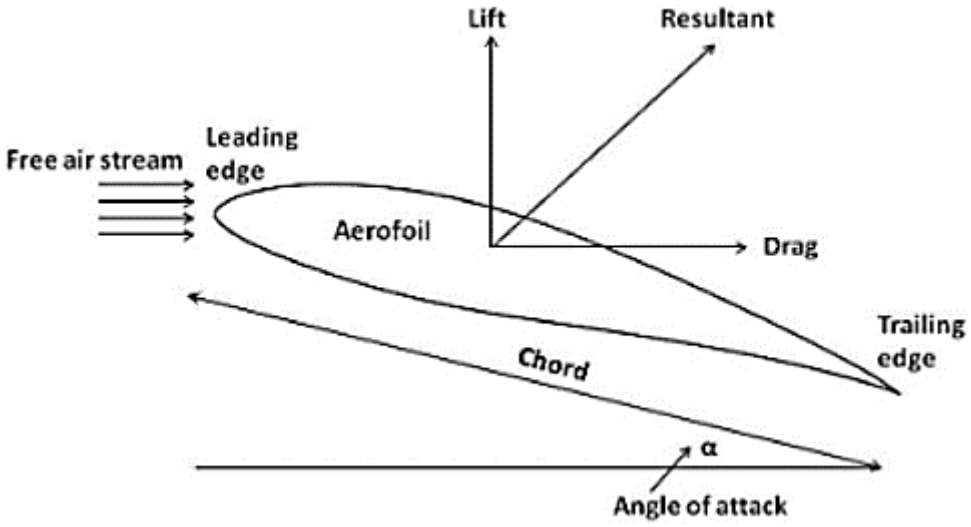

Figure 2. 2: Forces acting on a typical airfoil section (Charan Panigrahi and Mishra, 2014)

The study of (Petinrin and Onoja, 2017) computationally predicted how the drag coefficient, lift coefficient and drag polar over the NACA 4412 airfoil vary with angles of attack and Reynolds number. ANSYS Fluent was used to solve various equations governing the flow such as the continuity equation, the Reynolds Averaged Navier-Stokes equation and the turbulence transport equation. In this study, the flow was taken as incompressible, steady and two-dimensional. Simulations were run for angles of attack ranging from -10° to 18° with an interval of 2° and for a Reynolds number range of 1.0×10^6 to 13.0×10^6. Results revealed a steady variation within the pre-stall region between lift coefficient and angle of attack while a gradual increasing curve for the drag coefficients. Figure 2.3 shows the computational domain with boundary conditions used in the study.

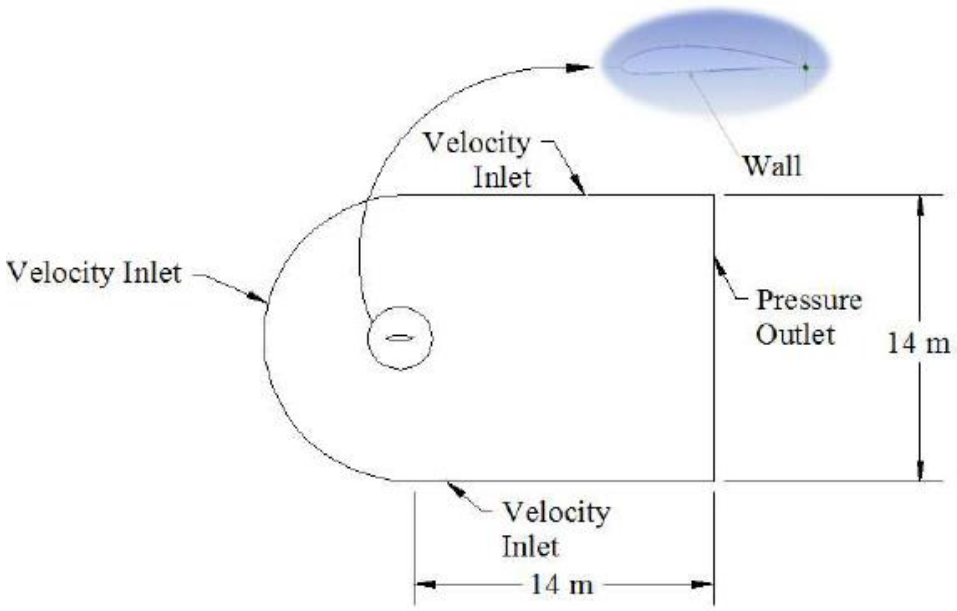

Figure 2. 3: Computational domain with boundary conditions (Petinrin and Onoja, 2017)

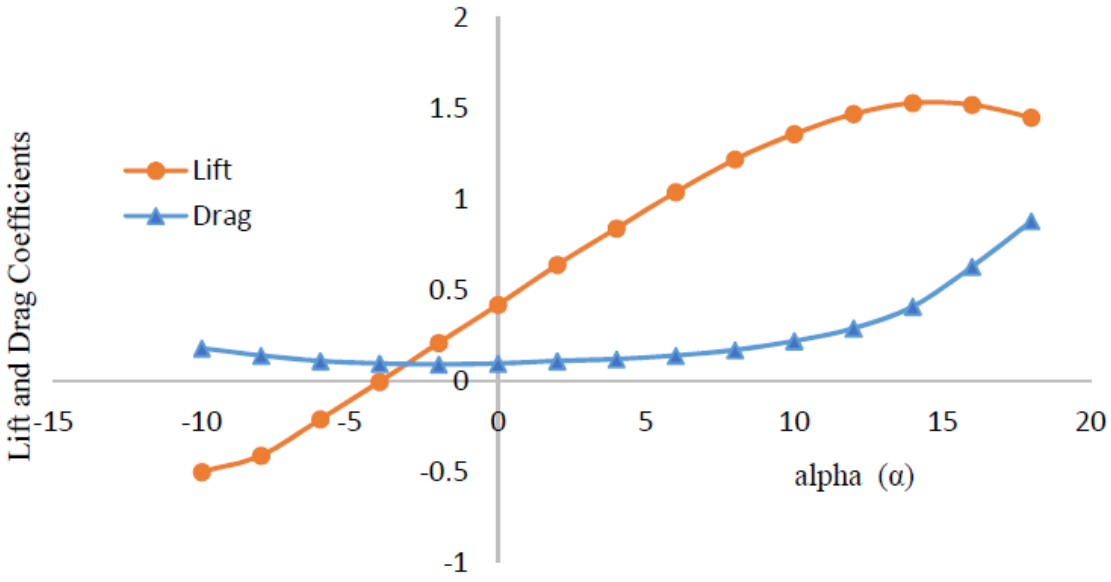

Figure 2. 4: Graph of lift and drag coefficient versus angle of attack at Re = 6×10^6 (Petinrin and Onoja, 2017)

The variation of lift and drag coefficient with angle of attack at a fixed Reynolds is shown in Figure 2.4. The lift coefficient increases steadily between the angles of attack -6° to 10°.

An obvious increase in lift coefficient was recorded with each increase in angle of attack up to 14°. This angle is the stalling angle of airfoil at that particular Reynolds number. Beyond this stalling angle, a gradual drop in the lift coefficient is observed. The angle of zero lift was recorded at -4°, meaning lift generated at this angle was zero. Negative values for lift coefficient indicates the action of net downward force on the airfoil.

Furthermore, the drag plot in Figure 2.4 shows a curve decreasing gradually before reaching a minimum angle of attack of -2°. Beyond this angle of attack, the drag coefficient continues to increase positively. Based on the mentioned lift and drag characteristics within the positive angles of attack, the lift generation is accompanied by drag generation.

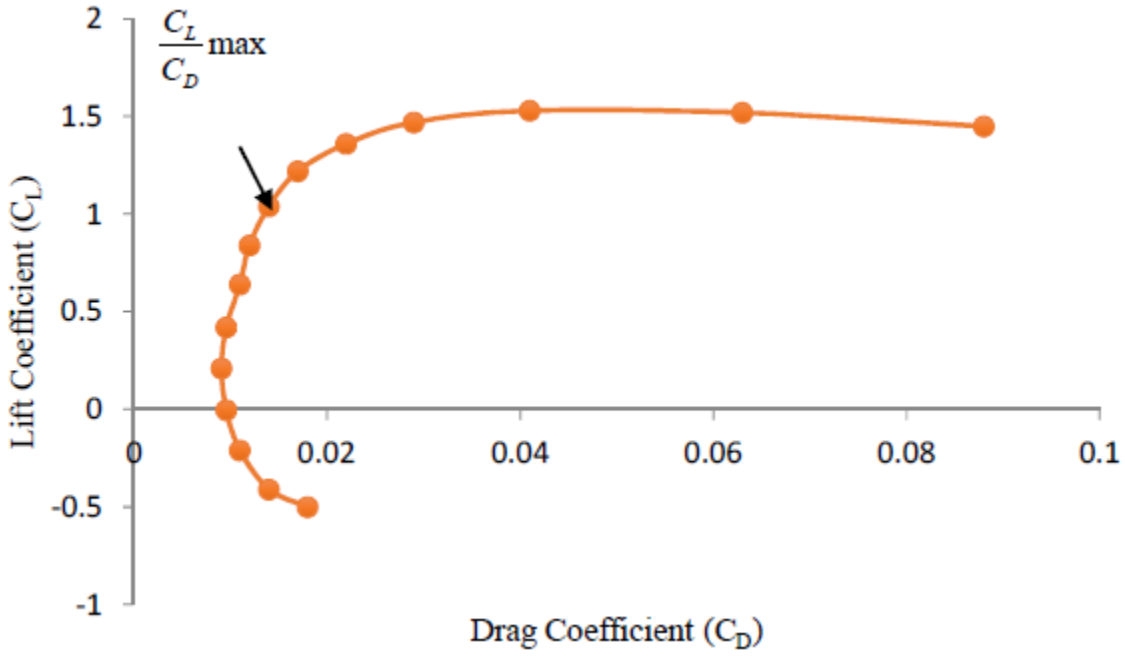

Figure 2. 5: The lift coefficient against drag coefficient, the Drag polar (Petinrin and Onoja, 2017)

Figure 2.5 which is a drag polar plot shows that the maximum ratio of lift to drag coefficient was achieved at an angle of attack of 6 °. This particular angle of attack indicates that the airfoil optimizes lift generation by generating the minimum amount of drag. If an airplane is flying in a steady flight at this angle, the total drag will be at minimum. At any angle of attack lower or higher, the lift-to-drag ratio will be decrease and thus increasing the total drag for a respective lift. Consequently, the fuel costs of the plane will cost more at this particular airspeed. It is also interesting to mention that the endurance and climb angle of jet-powered aircrafts are maximized when it is at an angle where lift-to-drag ratio is maximum.

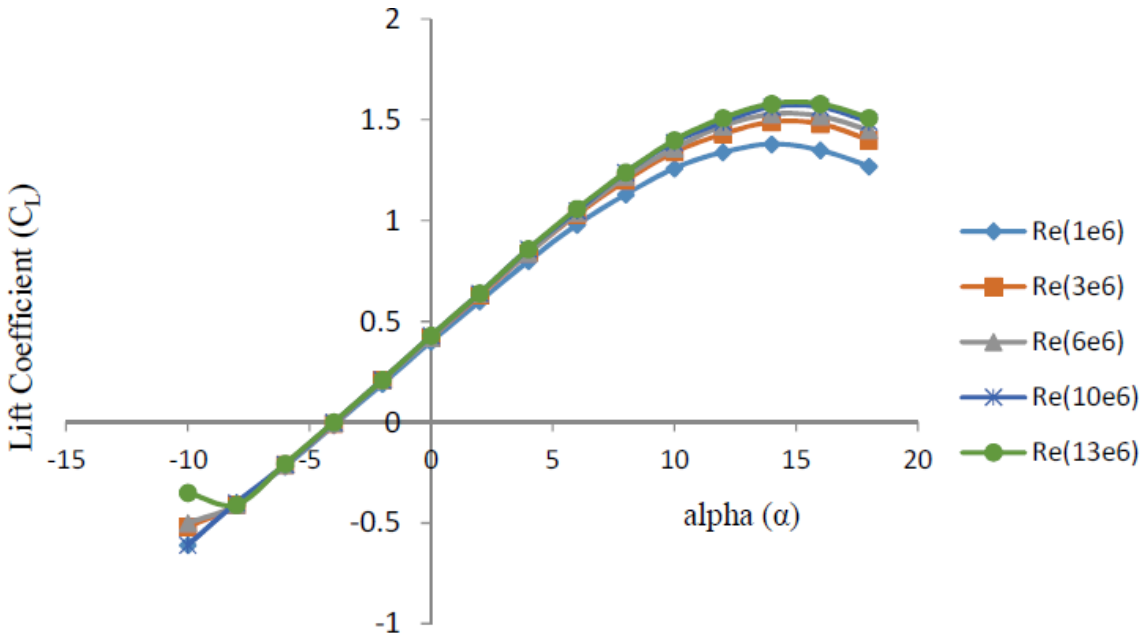

Figure 2. 6: The lift coefficient versus angle of attack at varying Reynolds numbers (Petinrin and Onoja, 2017)

The same study also shows the variation of lift coefficient with angle of attack at different Reynolds number in Figure 2.6. The increasing values of the lift coefficient reduced as the

Reynolds number is increased in the positive angle of attack. Also, there is no or obvious increase in the lift coefficient when the Reynolds number increases beyond 10×10^6.

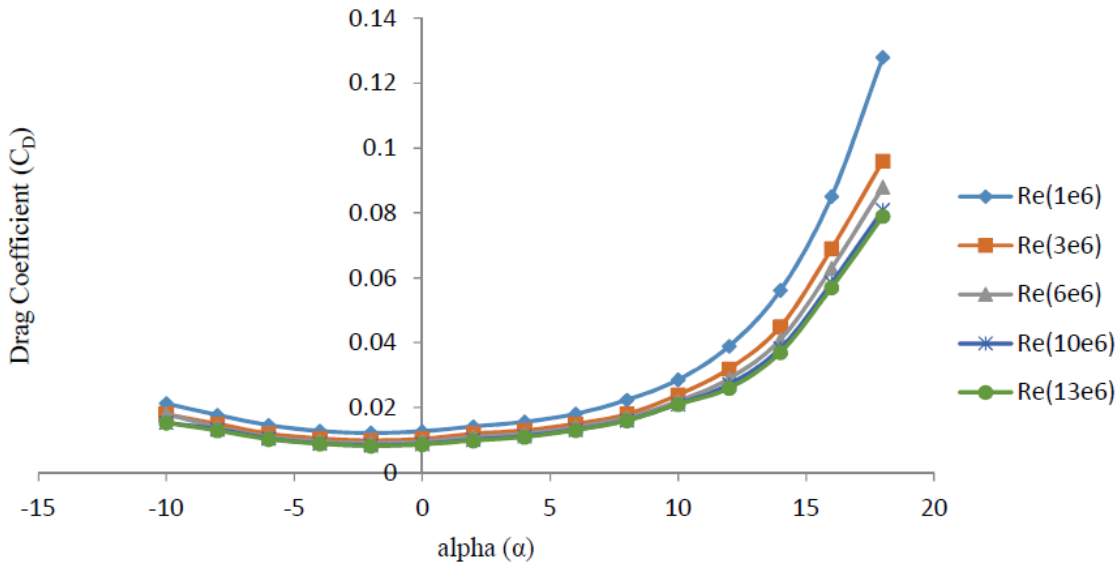

Figure 2. 7: The drag coefficient versus angle of attack at varying Reynolds numbers (Petinrin and Onoja, 2017)

As for the drag coefficient, the values are lower at higher Reynolds numbers for the range of angle of attack, as shown in Figure 2.7. When a higher Reynolds numbers is investigated, there is no significant difference between the drag coefficients.

The C_L/C_D or drag polar graph against the angle of attack at different Reynolds number for the same research is shown in Figure 2.8. The maximum drag polar is at $6\,°$ for all the Reynolds numbers listed. Also, the increase in drag polar reduces a little by little as the Reynolds number increases. Thus, the increment in drag polar is obviously low beyond Reynolds number of 10.0×10^6.

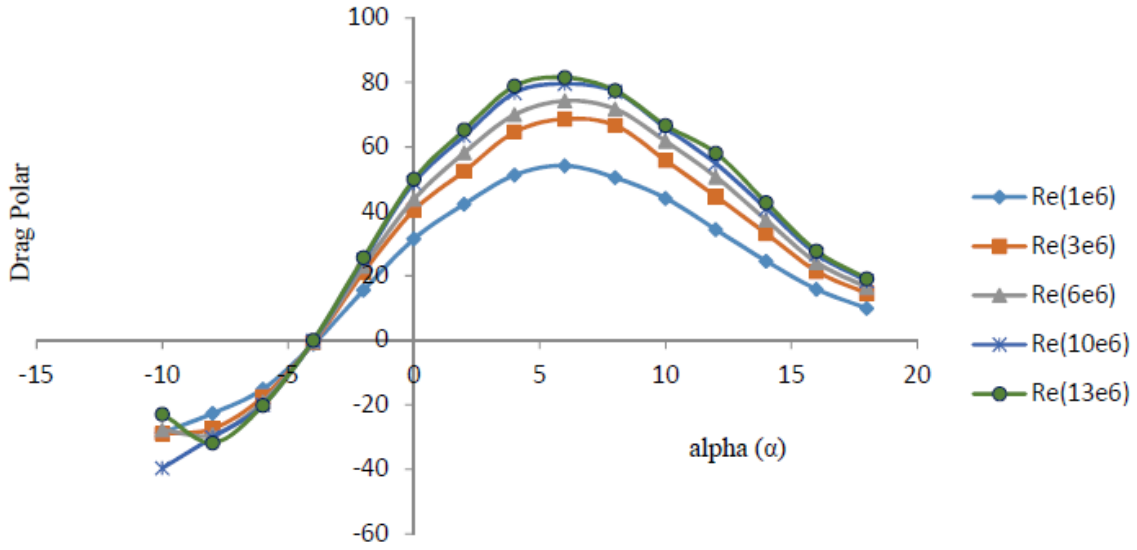

Figure 2. 8: The drag polar versus angle of attack at varying Reynolds numbers (Petinrin and Onoja, 2017)

Another experiment that involves the influence of angle of attack and the chord base Reynolds number on the lift and drag coefficients for NACA 0012 airfoil was conducted by (Mart ńez-Aranda et al., 2016). The experimental tests were performed with a closed circuit low speed wind tunnel with wind speed of 4 to 30 m/s, airfoil angle of attack ranging from 0 °to 35 °and the chord based Reynolds number can be obtained from Equation 2.1.

$$Re_c = U_\infty . c/v \tag{2.1}$$

Thus, four Reynolds numbers were used which include $3.3\times\ 10^4$, $6.67\times\ 10^4$, $1\times\ 10^5$ and $1.33\times\ 10^5$. Then the polar curve of C_L/C_D against angle of attack was plotted as shown in Figure 2.9. It is shown that the maximum C_L/C_D ratio increases with Reynolds numbers until the Reynolds number of $1\times\ 10^5$ is achieved. Beyond this Reynolds number, there is a variation in the increasing pattern of the curve and the respective maximum C_L/C_D value at

Reynolds number of 1.33× 10^5 begins to decrease with the chord based Reynolds number. This chord based Reynolds number is known as the critical Reynolds number.

From the same research, it is also observed that maximum C_L/C_D value for all the Reynolds numbers is found between angle of attack 10 ° to 12 °. In other words, the airfoil has the highest efficiency between 10 °to 12 °depending on the chord based Reynolds number.

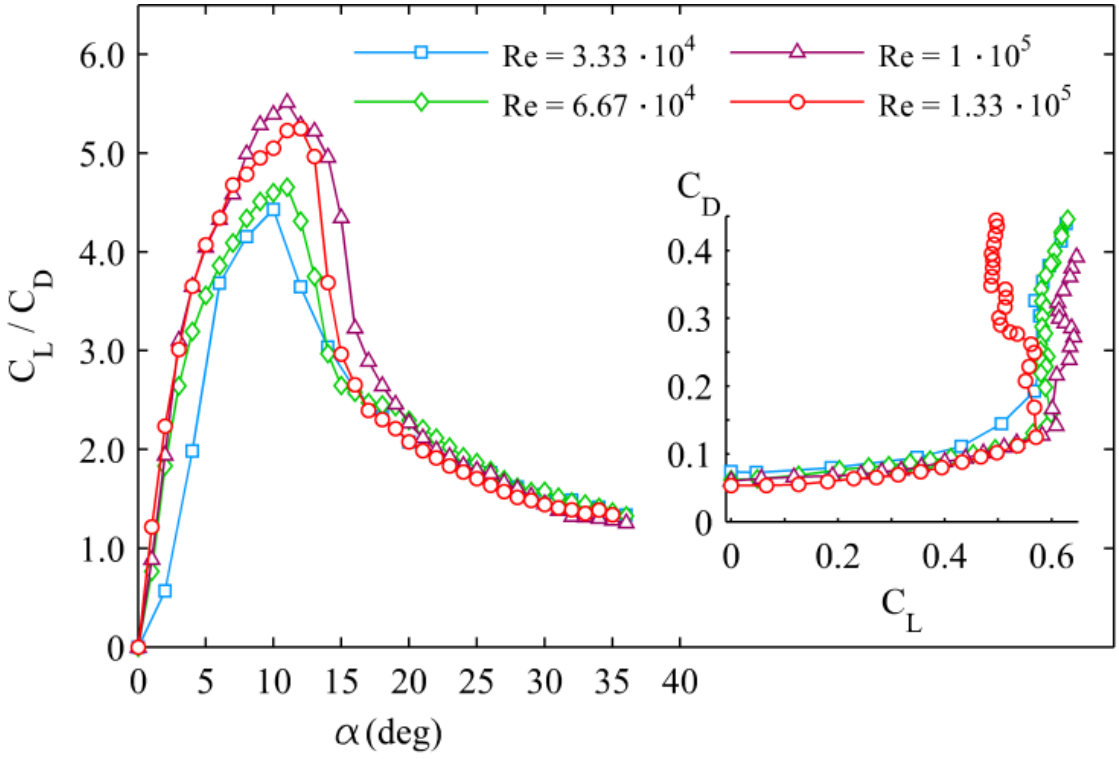

Figure 2. 9: Lift-Drag ratio C_L/C_D vs angle of attack α. The inset shows C_D vs C_L for all Reynolds numbers tested (Mart ńez-Aranda et al., 2016)

A numerical simulation was conducted by (Khan et al., 2017) to explore the effect of vibration frequency and amplitude. The flexible structure vibrated in a single mode located on the upper surface of the airfoil, as shown in Figure 2.10.

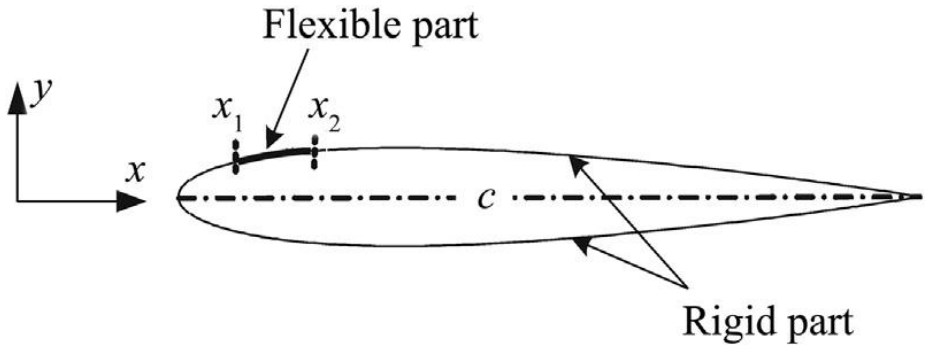

Figure 2. 10: Modeling of Local Flexible Airfoil (Khan et al., 2017)

The study was conducted for flow over NACA 0012 airfoil at 600≤ Re ≤ 3000 at a low angle of attack. The vibration frequency of the flexible structure, f_v at constant amplitude A_v is examined. Figure 2.11 shows the time history lift coefficient and the power spectra at Reynolds number of 1 000 and f_r=1. After the experiment, it showed that the vibration of flexible structure induced a secondary vortex that modified the pressure distribution and lift performance of the airfoil. The results also showed a complete synchronization happened when the vibration frequency of flexible structure equal to the natural frequency of the rigid airfoil (f_r=1). Also, the amplitude of lift coefficient oscillations depended on the Reynolds number. Vibration of flexible structure induced an additional vortex that caused the wake structure to be different from wake of rigid airfoil. In the presence of flexible structure, the average lift coefficient of the airfoil is increased by 4.75 % and 2.27 % at f_r=1 and 1.1 respectively.

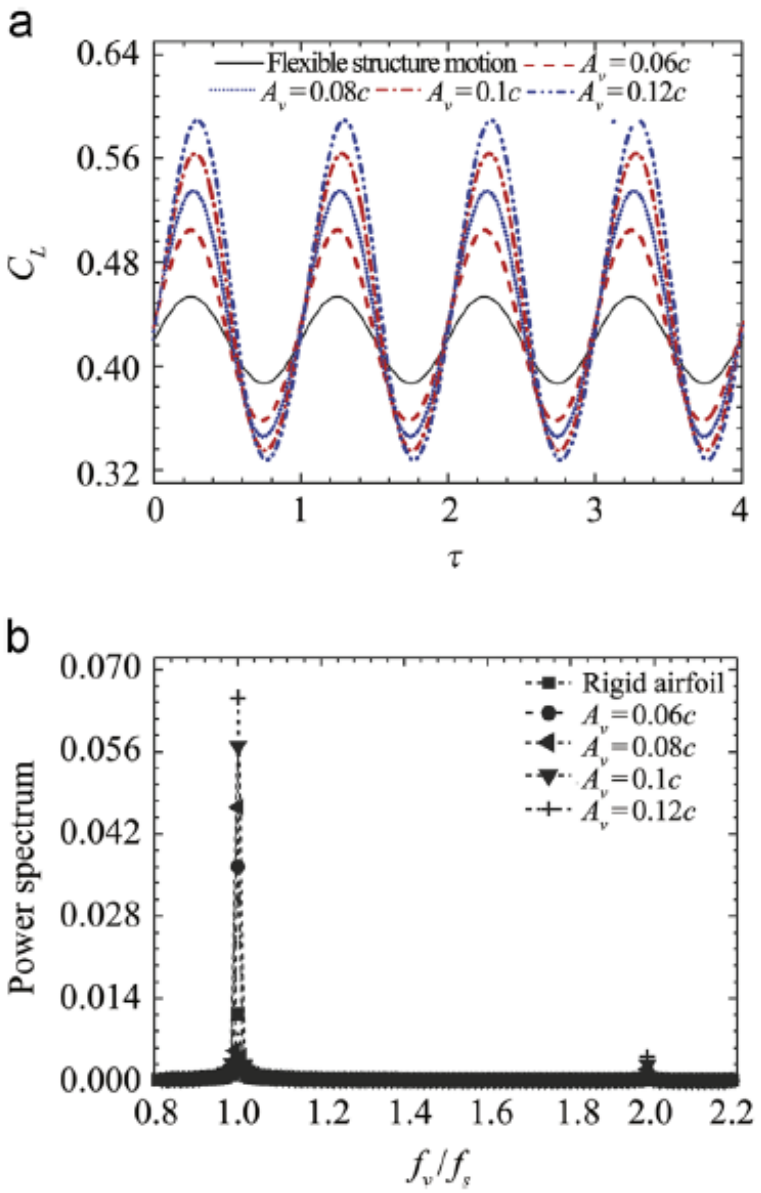

Figure 2. 11: (a) Time history lift coefficient (C_L) and (b) their power spectra at Re = 1 000 and f_r = 1 (Khan et al., 2017)

CHAPTER 3

METHODOLOGY

3.1 Experimental apparatus

3.1.1 NACA 4412 Airfoil Model

NACA 4412 airfoil model as shown in Figure 3.1 is used in this experiment to study the effect of vibration frequency on aerodynamic performance. Figure 3.2 shows the airfoil dimension where it is known that the length, l is 14.2 cm, chord length, c is 10 cm and the thickness, t is 1.3 cm.

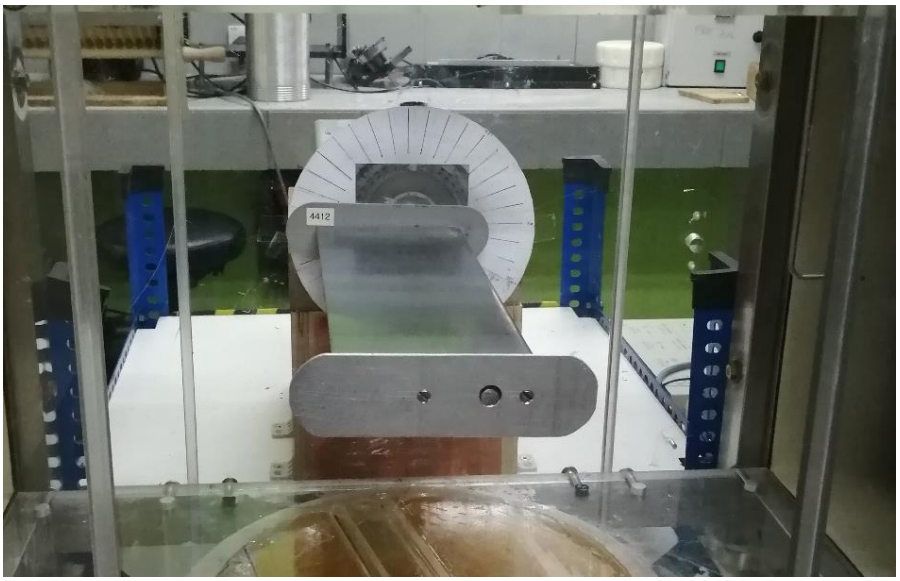

Figure 3. 1: NACA 4412 Airfoil Model

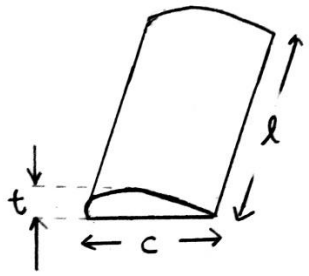

Figure 3. 2: Dimension of the NACA 4412 airfoil model

3.1.2 Open-circuit wind tunnel with bi-test-section

A wind tunnel is designed for a specific purpose and speed range. The model to be tested such as an airfoil will be put in the test section. The speed range of the tunnel depends on its design due to compressibility effects and the boundary layer formed by the walls. (Ghose et al., 2014)

As shown in Figure 3.3, the open circuit wind tunnel used in this experiment has 2 test sections in its body with an assembly of multiple components such as the intake section, test section, diffuser, axial fan and settling chamber. This project focuses on Test Section 2 where the NACA 4412 airfoil model will be installed in this section for the experiments. The schematic drawing and general dimensioning of the wind tunnel is shown in Figure 3.4.

Figure 3. 3: Set-up of open-circuit wind tunnel with bi-test-section

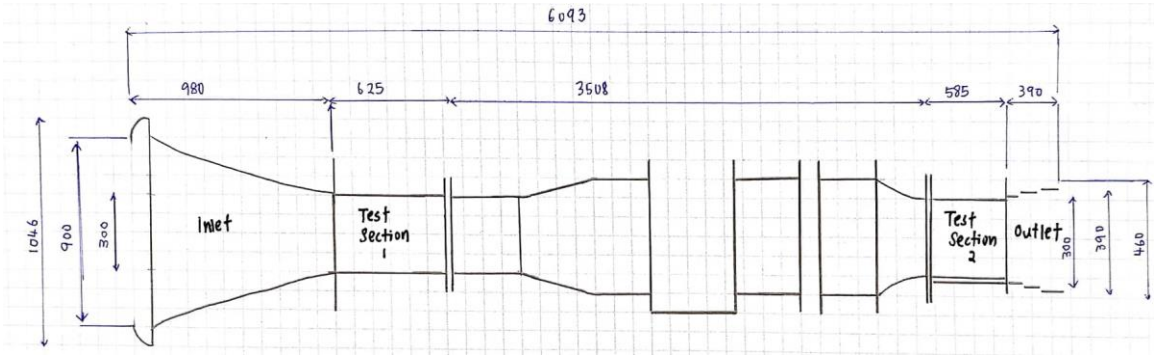

Figure 3. 4: Schematic drawing and general dimensioning (in mm) of the open circuit wind tunnel

The wind tunnel measures the aerodynamic forces and moments on the NACA 4412 airfoil model but in this research, only aerodynamic forces such as lift and drag are recorded for further investigation. The airfoil model is mounted in the tunnel on a force balance which in this research is the Data Acquisition (DAQ) electronic balance. The output from the electronic balance will be a signal that is related to the forces such as the lift and drag forces on the airfoil model (Hall, 2015b).

3.1.3 Data Acquisition (DAQ) Electronic Balance & Strain Gauge

Data acquisition is defined as a process of collecting or sampling signals that measure physical conditions before converting the samples into digital numerical values manipulated by a computer. A data acquisition system is known as a collection of equipment and circuits used to capture data from various sensors when testing or monitoring conditions in a specific product or system (Frenzel, 2018). As mentioned, the airfoil model is mounted in the tunnel on the Data Acquisition (DAQ) electronic balance. When the wind tunnel is switched on to induce the air flow, the forces that are acted on the airfoil model will be detected by the strain gauge which is then connected to this Data Acquisition (DAQ) Electronic Balance.

The output from the electronic balance will be a signal that is related to the forces such as the lift and drag forces on the airfoil model. The electronic balance will be calibrated and the method of calibration will be further discussed later. The force measurements also require a post-processing to account for Reynolds number effects on the airfoil model during testing (Hall, 2015b).

For both case of rigid airfoil and vibrating airfoil, the respective lift and drag forces acted on the airfoil model with varying Reynolds number and angles of attack will then be shown in the computer display.

Figure 3.5 shows the KYOWA PCD-300A used in the research while Figure 3.6 shows the strain gauge that is a device used to measure strain on the airfoil. Figure 3.7 shows the overall setup of DAQ Electronic Balance in recording the data.

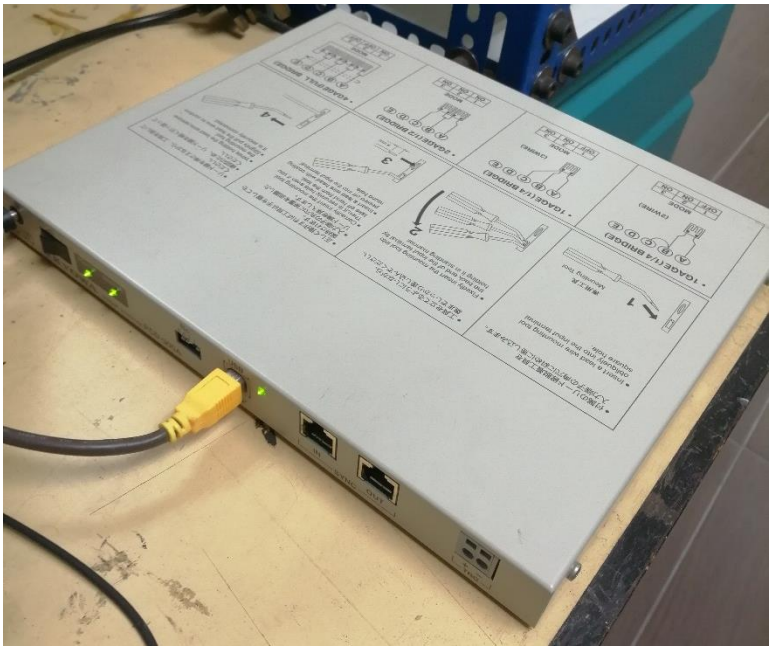

Figure 3. 5: KYOWA PCD-300A

Figure 3. 6: Strain Gauge

Figure 3. 7: Overall setup of DAQ Electronic Balance in recording the data

3.1.4 High Speed Vibration Motor 0716

The vibration motor induces vibration and thus provides vibration frequency to the NACA 4412 airfoil model. Figure 3.8 shows the high speed vibration motor that is used in the experiment. As shown in Figure 3.9, the vibration motor is attached to the middle part of the airfoil model to achieve effective vibration. The motor will not be needed for the case of rigid airfoil.

Figure 3. 8: High Speed Vibration Motor 0716

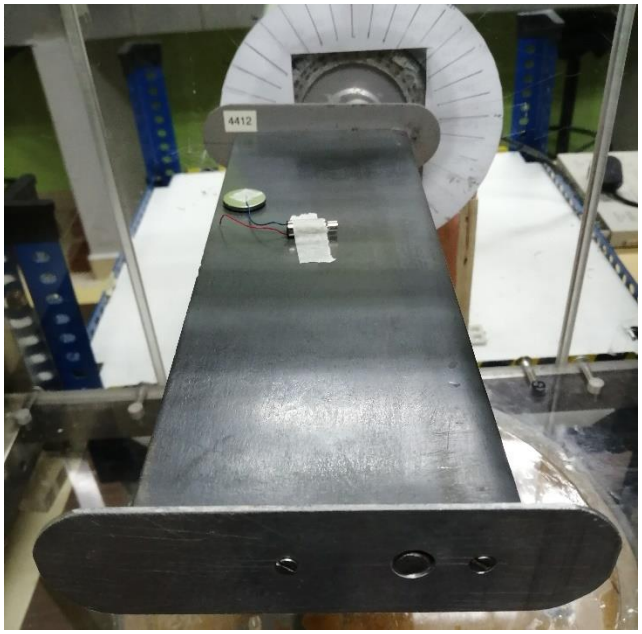

Figure 3. 9: A vibration motor is attached on the airfoil model

3.1.5 Victor 816B Digital Anemometer

When using the open circuit wind tunnel, it is needed to adjust the blade rotational speed. Table 3.1 shows the blade rotational speed with respect to the air speed of the open circuit wind tunnel.

Table 3. 1: Blade Rotational Speed and Air Speed of Test Section 2 for Open Circuit Wind Tunnel

Rotational Speed (rpm)	Air Speed (m/s)
260	0
520	1.28
780	4.43
1040	6.89
1300	8.08
1560	9.98

However, it is not easy to adjust the rotational speed of the blade to a whole number such as 520 rpm, the adjusted speed might be jumping for instance from 519.8 rpm to 523.9 rpm, making an air speed that is not equal to 1.28 m/s as expected. Thus, a more accurate tool is used to obtain the air speed coming from the wind tunnel which is a digital anemometer.

Figure 3.10: Victor 816B Digital Anemometer

Figure 3.10 is the Victor 816B Digital Anemometer is an instrument that measures wind speed and temperature. In this research, it is used to measure the air speed coming from the wind tunnel inlet. Figure 3.11 shows the method used to measure the air speed of wind tunnel using the digital anemometer, the air speed will be shown in the screen of the anemometer.

Figure 3. 11: Using a digital anemometer to measure the air speed of wind tunnel

3.2 Calibration

Before the data recording of the experiment, it is a must to perform calibration on the wind tunnel. The purpose of doing this is to check the accuracy of the measurement obtained from the open circuit wind tunnel so that a more accurate result will be obtained at the end of the experiment. As known, the accuracy of any measuring devices degrades over time and is usually caused by normal wear or tear. Thus, calibration improves the accuracy of the

measurement. The calibrations needed to conduct in this experiment include the lift and drag calibration.

3.2.1 Calibration Procedure

The setup for lift calibration is shown in Figure 3.12 where a weight is put in the middle part of the NACA 4412 airfoil model.

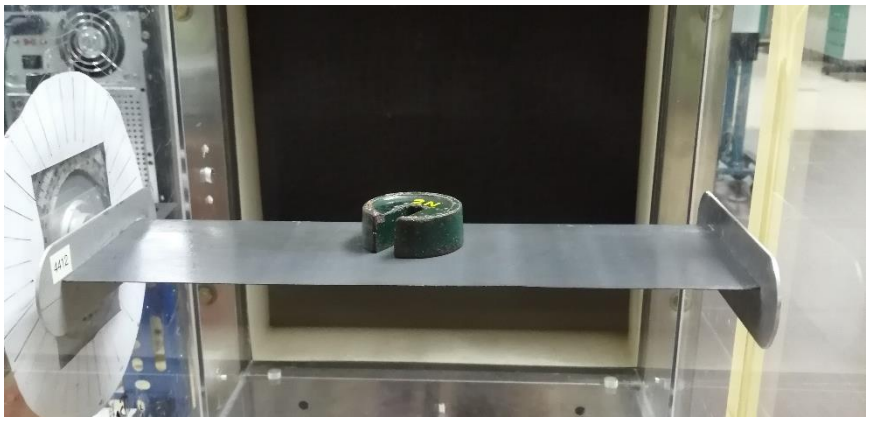

Figure 3. 12: Setup of lift calibration where a 2N-weight is put in the middle of the airfoil model

For the lift calibration, firstly, the airfoil needs to be at zero angle of attack to be calibrated. The ‘balance’ button must be clicked at the right top part of the PCD-30A Control Software tab to balance the reading of the lift and drag at zero angle of attack of airfoil. The red ‘stop’ button will be clicked before putting a 2N-weight on the middle of the airfoil model for lift calibration. By clicking the ‘Set CH Conditions’, a tab appears showing all the CH conditions. Since PCD 2 is connected from the DAQ to the computer, CH5, 6, 7 and 8 are shown in the CH conditions where CH 6 and CH 7 is lift and drag measurement respectively in this experiment. Both CH 6 and 7 are ticked in the ‘measurement’ column as well as the ‘balance’ column to conduct the calibration. Then, click ‘OK’ to exit from the ‘Set CH